Structural, Rotational, Vibrational, and Electronic Properties of Carbon Cluster Anions C_n^- ($n = 3-13$)

M. G. Giuffreda, M. S. Deleuze,* and J.-P. François

Limburgs Universitair Centrum, Institute for Materials Science (IMO), Departement SBG, Universitaire Campus, B-3590 Diepenbeek, Belgium

Received: October 18, 2001; In Final Form: May 13, 2002

The structural, rotational, and vibrational properties of C_n^- clusters ($n = 3-13$) have been investigated by means of density functional theory (DFT/B3LYP) and, whenever possible, coupled cluster (CC) theory along with the aug-cc-pVDZ basis set. These properties are compared with those of their neutral counterparts and of the corresponding cations. The linear and merely cumulenic chains undergo a substantial increase of the bond-length alternation and an increase of size upon adiabatic electron attachment. In addition, most chains (C_5, C_7, C_8, C_9, and C_{10}) become slightly bent in their anionic form because of Renner−Teller effects. The structural outcomes of such processes on carbon rings are far more varied and can be rationalized solely through a topological analysis of the frontier orbitals. Both for the linear and cyclic species, IR spectra and rotational moments provide specific markers of these complex structural variations. Closed anionic clusters such as C_5^-, C_9^-, and C_{13}^- are even-twisted cumulenic rings. The highest occupied levels of these rings relate to orbitals with a particularly exquisite bonding pattern, which explains, among other effects, significant departures from planarity. It has been noticed that *d* diffuse functions are essential for a sound description of the Renner−Teller distortions of C_n^- chains and of the nonplanar nature of the C_{13}^- ring. The linear anionic chains exhibit a much stronger IR activity, as well as a systematically greater propensity to bind an extra electron, than the cyclic isomers. Among the rings, the adiabatic electron affinities (AEAs) of the C_9 and C_{13} species are strikingly high, whereas the lowest value of AEA coincides with the cumulenic C_{10} species. For the anionic chains and the larger rings, the most intense IR absorption lines have vibrational frequencies ranging from 1600 to 2200 cm^{-1}.

1. Introduction

Carbon cluster anions have been detected and produced in many different chemical and physical environments using a great variety of techniques.[1,2] In the late 1980s, Yang and co-workers measured the ultraviolet photoelectron spectra (UPS) of mass-selected carbon cluster anions extracted from a pulsed supersonic beam with sizes ranging from C_2^- to C_{84}^-.[3,4] The electronic and vibrational properties of these clusters have thereafter been investigated in more detail using mass selection techniques combined with anion photoelectron spectroscopy techniques[5−8] as well as resonant-enhanced multiphoton electron-detachment spectroscopy (REMPED) in the gas phase,[9,10] infrared spectroscopy,[11−14] and matrix isolation spectroscopy.[15−20]

Structural analysis of C_n^- clusters is a very challenging research topic. Photoelectronic studies suggest the existence of linear chains from C_2^- to C_9^- and of monocyclic rings from C_{10}^- to C_{29}^-.[4,6] Ion mobility measurements[21] seem to indicate that linear isomers exist only from C_5^- to C_9^-, whereas both linear and cyclic isomers are simultaneously observed from C_{10}^- to C_{30}^-. Further mass spectrometric studies on C_n^- ($n = 4-100$) species[22] suggest that a fullerene structure is preferred for anionic clusters of the size of C_{33}^- and larger. These measurements also indicate a predominance of the even clusters with respect to the odd ones from C_4^- to C_{13}^-, whereas the odd clusters appear to be the most abundant species from C_{14}^- to C_{33}^-. In this study,[22] linear and monocyclic structures have been suggested for both of these sets. However, as pointed out by Kohno et al.,[8] the presence and detection of linear or cyclic C_n^- clusters seem to be strongly dependent on the experimental conditions. Specifically, in laser vaporization experiments on graphite surfaces,[8] a low-fluence laser excitation mainly causes desorption and decomposition of large hot particles. In this case, the decomposition processes seem to favor the formation of monocyclic carbon anions with sizes ranging from C_{10}^- and C_{18}^-. It has been suggested that in such conditions the anion formation is mostly due to electron attachments to the neutral systems after cooling, which would explain the similar mass distributions between the neutral systems and the anions. However, the use of a higher fluence implies a further atomization of the targets, thus favoring the formation of small linear structures.

Because the structure and energetics of negatively charged carbon clusters are still largely unresolved issues on the experimental side, research in this field has unsurprisingly motivated a considerable number of theoretical investigations. However, most of the calculations reported on C_n^- species concern the linear isomers.[23−35] The only cyclic C_n^- structures that have been studied so far are C_3^-,[11] C_4^-,[11,36−38] C_6^-,[11,31] C_7^-,[32] and C_{11}^-.[34] These theoretical studies have been performed merely on the basis of calculations at the self-consistent field (SCF) restricted Hartree−Fock (RHF) and restricted open-shell Hartree−Fock (ROHF) levels. Of relevance to the present work is a previous systematic investigation of the molecular structure of chains ranging from C_2^- to C_{10}^- using ROHF and single-

* Corresponding author. E-mail: deleuze@luc.ac.be.

10.1021/jp0211436 CCC: $22.00
Published on Web 08/15/2002

point coupled-cluster (CC) methods.[24] In that work, geometry optimizations were also performed at different levels of theory for some linear clusters. More specifically, for C_4^-, optimized structures have been calculated[24] at the UHF-MBPT(2), UHF−SDQ-MBPT(4), and UHF−CCSD levels. For C_5^-, further data are available[24] at the UHF-MBPT(2) and UHF-SDQ-MBPT(4) levels. For C_6^-, calculations have been carried out at the UHF-MBPT(2),[24,39] RCCSD(T), RCCSD-T[27], and DFT/B3LYP[31] levels of theory. Finally, for C_7^- and C_8^-, RCCSD, RCCSD-(T),[29,33] or RCCSD-T[28] calculations are also reported. Geometries and vibrational frequencies of cyclic C_3^-, C_4^-, and C_6^- at the B3LYP/6-31G* level are given in ref 11. In this latter work, no stable geometries for cyclic C_5^-, C_7^-, C_8^-, and C_9^- clusters could be located.

The early photoelectron measurements of Yang and coworkers on carbon clusters ranging from C_2^- to C_{29}^- were focused, in particular, on the determination of the electron-detachment energies of these species[3] and, conversely, the electron affinities of their neutral counterparts. Quite naturally, these properties, as well as other one-electron binding energies such as ionization potentials, gave rise, on the theoretical side,[23−25] to extensive investigations by means of indirect (two-step) calculations at the above-mentioned levels on small carbon clusters and their cations or anions. In this way, the vertical and adiabatic electron affinities of carbon chains ranging from C_2 to C_{10} [24,26] and of the C_4 ring[36] could be determined at various levels (ROHF, MBPT(2), CCSD(T)) using structures optimized at the SCF or (for the C_4 and C_5 rings) MBPT(2) levels.[24,40,41] The vertical electron affinities of small odd-membered C_{2n+1} ($n = 1-6$) carbon chains,[25,40−42] or of the C_4 carbon ring,[38] have also been determined by one-shot one-electron propagator calculations on structures optimized at the HF and MBPT(2) levels. In general, from these studies on the linear anions, it has been concluded that adding an electron to the neutral species increases the bond-length alternation in comparison with that of the neutral species. However, it is worth reminding that for strongly correlated systems such as cumulenic carbon chains or rings the HF wave function is very unstable toward geometrical distortions. More specifically, the lack of correlation at the HF level often results in a strong overestimation of the alternation of bond lengths. It has also been observed[2] that MBPT(2) (or, equivalently, MP(2)) is not a reliable level for treating carbon clusters in general.

The study of anionic species with density functional theory[43] (DFT) has been a matter of discussion in the past because of the problem of the electron self-interaction,[44,45] which is responsible for the erroneous prediction that some known negatively charged species are unstable against electron detachment. However, several groups[30,46−52] have shown that with pure and hybrid DFT methods accurate adiabatic electron affinities can be predicted for a wide range of molecular systems. The interested reader is in particular referred to evaluations[52] of the electron affinities of challenging species such as F and F_2 with a variety of functionals and extremely large, diffuse basis sets, in addition to the evaluation of the behavior of a known unbound system, Ne^-. It has also been shown that accurate equilibrium geometries and harmonic vibrational frequencies of anionic species can be predicted with such methods.[46] Furthermore, DFT computations (eight medium-sized carbon-containing molecules[30]) by means of the B3P86, BLYP, and B3LYP functionals in conjunction with a double-ζ basis set with polarization and diffuse functions provide adiabatic electron affinities that do not deviate from experiment by more than 0.2 eV.

In this work, we report an exhaustive study of the structural, rotational, and vibrational properties of carbon cluster anions C_n^- with $n = 3-13$ using density functional theory,[43] along with Becke's three-parameter Lee−Yang−Parr (B3LYP) functional.[53,54] Whenever possible, the CCSD(T) method (coupled-cluster ansatz including single and double excitations and a perturbative estimate of triple excitations)[55−57] is also employed to assess by means of single-point calculations the accuracy of relative energies between the cyclic and linear carbon clusters. Also, infrared (IR) absorption activities, vibrational zero-point energies, and harmonic frequencies have been calculated at the DFT/B3LYP level. The latter are computed, in particular, to identify specific markers of the structural changes that occur when an electron is added to the neutral carbon clusters.

The interested reader is further referred to refs 58 and 59 for similar investigations of the relative energies and the structural, rotational, and vibrational properties of the corresponding neutral carbon clusters and cations, which enable a complete understanding of the adiabatic ionization processes on C_n ($n = 3-19$) clusters.

2. Methods

Undoubtedly, theoretical investigations of highly reactive clusters, such as carbon chains and rings, must treat electron correlation in the ground-state wave function. Therefore, a reliable analysis requires the use of methods that are able to account for electron correlation quantitatively and, at the same time, can still be applied to large systems with reasonable computational costs. At present, DFT methods along with a nonlocal hybrid functional such as B3LYP[53,54] represent one of the best options that may be used reliably to overcome the deficiencies of the HF model in giving correct molecular structures and vibrations. As shown in several instances,[59,60] the DFT/B3LYP level provides structures and vibrations of a quality comparable to those obtained at the CCSD(T) level, with the advantage of a much lower computational cost.

To give a sufficient flexibility to the electron wave function, more specifically, to enable a consistent description of the binding of an extra electron at relatively large molecular distances, an augmented Dunning's correlation-consistent polarized valence double-ζ (aug-cc-pVDZ) basis set[61] has been used for all DFT(B3LYP) computations described in the article. It consists of a [4s3p2d] contraction of a (9s4p1d + 1s1p1d) primitive set. The initial structural guesses regarding the optimization of the structure of the carbon cluster anions were the B3LYP/cc-pVDZ geometries of the neutral systems.[58]

The CCSD(T) energies presented in the forthcoming analysis are the results of single-point calculations with all electrons correlated using the aug-cc-pVDZ basis set. These calculations have been completed by means of the MOLPRO program package,[62] whereas the DFT calculations presented in this work have been carried out using Gaussian 98.[63] Numerical integration of the functional was carried out using the Gaussian 98 default grid, which is composed of 75 radial shells with 302 angular points per shell.

3. Results and Discussion

3.1. Structural Properties of Linear Clusters. The first purpose of this study of linear carbon cluster anions is to provide a calibration of the method (i.e., B3LYP/aug-cc-pVDZ) by comparison with higher or comparable levels of theory. Upon inspection of the geometries and adiabatic electron affinities, it appears that the B3LYP functional, combined with the augmented cc-pVDZ basis set, is appropriate for studying carbon cluster anions. According to Watts and Bartlett[26] and Brown et al.,[30] the use of basis sets that include diffuse functions is

unavoidable if reliable values for the adiabatic electron affinities (AEAs) are to be obtained. Test calculations have been performed on the linear and cyclic isomer of C_8^- using B3LYP together with the cc-pVDZ and aug-cc-pVDZ basis sets to clarify the effect of the basis set. By comparing the structures obtained with the two different basis sets, we have noticed that the variations of the bond lengths due to the inclusion of the diffuse functions are, on average, around 0.001 Å for the linear anion and 0.002 Å for the cyclic anion. An AEA value of 4.15 eV is obtained at the B3LYP/aug-cc-pVDZ level for the linear isomer of C_8, in good agreement with the experimental value of 4.379 ± 0.006 eV; however, the AEA reduces to 3.84 eV when the B3LYP/cc-pVDZ approach is used. A similar observation can be made for the cyclic C_8 species; AEA values of 2.55 and 2.01 eV are obtained with the aug-cc-pVDZ and cc-pVDZ bases, respectively. It appears, therefore, that the impact of diffuse functions is enhanced when the lowest unoccupied molecular orbital approaches the continuum, leading to AEA values close to zero. With electron-detachment energies in general larger than 2 eV, C_n^- clusters are strongly bound species that can satisfactorily be described by an aug-cc-pVDZ basis set.

The optimized structures of the C_n^- chains in the range $n = 3-10$ are described in their doublet ground states in Table 1. For comparison purposes, the structure of the neutrals in their singlet or triplet ground states is also presented. For the sake of convenience in the analysis, the bond-length alternations are given in Table 2. C_n chains in their neutral form are essentially regular (i.e., cumulenic) systems, which tend to show stronger bond-length alternations when an electron is removed[59] or added (Table 2). The structural deformations induced upon electron attachment are overall more pronounced for the chains with an even number of atoms than for the odd-membered ones. As was noted previously for the adiabatic ionization process,[59] the amplitude of the distortions decreases rapidly with the size of the chains, reflecting the enhanced delocalization of canonical orbitals.

The results obtained for bond lengths at the B3LYP/aug-cc-pVDZ level are in line with the trends inferred from previous calculations at lower levels of theory. However, the extent of the bond-length alternation is markedly reduced compared with the results obtained by Watts and Bartlett at the ROHF level[23,26] (see Table 1 for a comparison). This feature is typical of large and low band gap one-dimensional systems, for which inclusion of electron correlation in the ground-state wave function is necessary to prevent or limit a Peierls distortion of their structure at the HF level.[64]

A comparison of our results with those obtained by Schmatz et al. for C_3^-, C_4^-, C_6^-, C_7^-, and C_8^- [27-29] (see Table 1) shows that the bond lengths calculated at the B3LYP/aug-cc-pVDZ level are in very good agreement with those obtained from high-level RCCSD(T)/cGTOs calculations and seem to be overestimated on average by 0.004 Å. Interestingly, the agreement is not as good with the results obtained previously for C_6^- at the MBPT(2)/6s4p1d level[39] and for C_5^- at the MBPT(2)/3s3p1d[41] level, where the bond lengths are systematically overestimated by a few hundredths of an Å compared with those presented here. From previous studies on carbon clusters,[2,65] we consider the DFT(B3LYP) scheme to be superior to the MBPT(2) level in structural investigations on such species. The present comparison confirms this point.

Linear carbon anions C_n^- with $n = 6-9$ have been also studied by Brown and co-workers[30] at the B3LYP/DZP++ level of theory. For comparison purposes, these results have also been included in Table 1. The bond lengths calculated with the DZP++ basis set are on average 0.004 Å longer than those obtained in this study using the aug-cc-pVDZ basis set.

When considering the results obtained for the C_5^-, C_7^-, C_8^-, C_9^-, and C_{10}^- chains, the effect of the basis set on the bond and torsion angles appears to be rather strong. In the literature,[24,26-30,35,39,41,58] these chains have always been predicted to be linear structures of $D_{\infty h}$ symmetry with a $^2\Pi_u$ or $^2\Pi_g$ ground state. This conclusion is the result of geometry

TABLE 1: Geometries of the Linear C_n^- ($n = 3-10$) Anions at the B3LYP/aug-cc-pVDZ Level

C_3^-	
$^2?$ ($D_{\infty h}$)	1.315
$^2\Pi_g$ ($D_{\infty h}$) ROHF/DZP[a]	1.301
$^2\Pi_g$ ($D_{\infty h}$) RCCSD(T)/cGTOs[b]	1.307
$^1\Sigma_g^-$ ($D_{\infty h}$) neutral	1.301
C_4^-	
$^2\Pi_g$ ($D_{\infty h}$)	1.284, 1.344
$^2\Pi_g$ ($D_{\infty h}$) ROHF/DZP[a]	1.265, 1.349
$^2\Pi_g$ ($D_{\infty h}$) RCCSD/cGTOs[b]	1.277, 1.336
$^3\Sigma_g^-$ ($D_{\infty h}$) neutral[c]	1.319, 1.299
C_5^-	
$^2A'$ (C_s)	1.293, 1.308 $\theta_{123} = 177.52$, $\theta_{234} = 175.10$
$^2\Pi_u$ ($D_{\infty h}$) MBPT(2)/3s3p1d[d]	1.319, 1.326
$^2\Pi_u$ ($D_{\infty h}$) SDQ-MBPT(4)/5s3p1d[e]	1.293, 1.317
$^2\Pi_u$ ($D_{\infty h}$) CCSD(T)/cc-pVTZ[e]	1.293, 1.307
$^2\Pi_u$ ($D_{\infty h}$) ROHF/DZP[a]	1.269, 1.309
$^1\Sigma_g^+$ ($D_{\infty h}$) neutral[c]	1.296, 1.291
C_6^-	
$^2\Pi_u$ ($D_{\infty h}$)	1.282, 1.332, 1.260
$^2\Pi_u$ ($D_{\infty h}$) ROHF/DZP[a]	1.258, 1.340, 1.237
$^2\Pi_u$ ($D_{\infty h}$) MBPT(2)/6s4p1d[f]	1.293, 1.341, 1.290
$^2\Pi_u$ ($D_{\infty h}$) RCCSD(T)/cGTOs[g]	1.281, 1.332, 1.259
$^2\Pi_u$ ($D_{\infty h}$) B3LYP/DZP++[h]	1.285, 1.338, 1.263
$^3\Sigma_g^-$ ($D_{\infty h}$) neutral[c]	1.309, 1.296, 1.283
C_7^-	
^2A (C_2)	1.287, 1.315, 1.285 $\theta_{123} = 178.64$, $\theta_{234} = 177.45$
$^2?$ ($D_{\infty h}$) ROHF/DZP[a]	1.261, 1.321, 1.270
$^2\Pi_g$ ($D_{\infty h}$) RCCSD(T)/cGTOs[b]	1.286, 1.314, 1.283
$^2\Pi_g$ ($D_{\infty h}$) B3LYP/DZP++[h]	1.290, 1.319, 1.289
$^1\Sigma_g^+$ ($D_{\infty h}$) neutral[c]	1.296, 1.295, 1.281
C_8^-	
$^2A_2$ (C_{2v})	1.281, 1.329, 1.260, 1.320 $\theta_{123} = 178.63$, θ_{234}=177.53, $\theta_{345} = 177.93$
$^2?$ ($D_{\infty h}$) ROHF/DZP[a]	1.275, 1.337, 1.234, 1.332
$^2?$ ($D_{\infty h}$) RCCSD(T)/cGTOs [g]	1.281, 1.329, 1.258, 1.321
$^2\Pi_g$ ($D_{\infty h}$) B3LYP/DZP++[h]	1.284, 1.333, 1.263, 1.326
$^3\Sigma_g^-$ ($D_{\infty h}$) neutral[c]	1.305, 1.297, 1.282, 1.289
C_9^-	
^2A (C_2)	1.284, 1.317, 1.276, 1.293 $\theta_{123} = 178.21$, $\theta_{234} = 176.50$, $\theta_{345} = 176.31$, θ_{456}=179.17
$^2?$ ($D_{\infty h}$) ROHF/DZP[a]	1.257, 1.327, 1.251, 1.292
$^2\Pi_u$ ($D_{\infty h}$) B3LYP/DZP++[h]	1.288, 1.322, 1.280, 1.298
$^1\Sigma_g^+$ ($D_{\infty h}$) neutral[c]	1.295, 1.298, 1.280, 1.285
C_{10}^-	
^2A (C_2)	1.281, 1.326, 1.261, 1.317, 1.261 $\theta_{123} = 178.66$, $\theta_{234} = 177.14$, $\theta_{345} = 176.37$, $\theta_{456} = 178.82$
$^2\Pi_u$ ($D_{\infty h}$) ROHF/DZP[a]	1.256, 1.336, 1.233, 1.331, 1.231
$^2\Pi_u$ ($D_{\infty h}$) estimated (see footnote *b* for details)	1.273, 1.331, 1.248, 1.316, 1.246
$^3?$ ($D_{\infty h}$) neutral	1.300, 1.300, 1.281, 1.290, 1.282

[a] Reference 24. [b] Reference 29. [c] Reference 58. [d] Reference 41. [e] Reference 26. [f] Reference 39. [g] References 27 and 28. [h] Reference 30.

TABLE 2: Successive Bond-Length Alternations (Å) in Linear Carbon Clusters in Their Ground States

species with an even number of atoms					
C_4^+	0.108				
C_4^-	0.060				
C_4	0.021				
C_6^+	0.079	0.047			
C_6^-	0.051	0.073			
C_6	0.014	0.012			
C_8^+	0.061	0.034	0.046		
C_8^-	0.048	0.069	0.060[a]		
C_8	0.008	0.015	0.007		
C_{10}^+	0.050	0.028	0.040	0.043	
C_{10}^-	0.045	0.065	0.056	0.056[a]	
C_{10}	0.0001	0.019	0.010	0.008	
species with an odd number of atoms					
C_3^+	0.000				
C_3^-	0.000				
C_3	0.000				
C_5^+	0.092	0.068	0.074		
C_5^-	0.016	0.0001	0.015[a]		
C_5	0.005	0.005	0.005		
C_7^+	0.056	0.041	0.061	0.084	0.100
C_7^-	0.028	0.030	0.000	0.030	0.028[a]
C_7	0.010	0.014	0.000	0.014	0.010
C_9^+	0.039	0.005	0.006		
C_9^-	0.033	0.041	0.017[a]		
C_9	0.003	0.018	0.006		

[a] Are not strictly linear (see text).

optimizations using a variety of approaches such as DFT, CCSD(T), and MBPT(4) in conjunction with basis sets such as 6-311G*, DZP, and DZP++. For these chains, as shown in Table 1, the B3LYP functional combined with the aug-cc-pVDZ basis set predicts slightly bent structures of C_s, C_2, or C_{2v} symmetry with a $^2A'$, ^2A, or $^2A_2$ ground state, whereas at the same level, the linear structures are found to possess one or two imaginary frequencies (C_5^-: 463i cm^{-1} and 284i cm^{-1}; C_7^-: 199i cm^{-1}; C_8^-: 447i cm^{-1} and 438i cm^{-1}; C_9^-: 202i cm^{-1}). At the B3LYP/aug-cc-pVDZ level, upon geometry optimizations performed using the tightest convergence criteria, these linear ($D_{\infty h}$) first-order or second-order saddle forms lie 0.33, 0.01, 0.05, and 0.20 kcal mol^{-1} above the bent energy-minimum forms, respectively. As suggested by Brown et al.,[30] such imaginary frequencies and thus the slight distortions seen from linearity in Table 1 for C_5^-, C_7^-, C_8^-, C_9^-, and C_{10}^- could be due to the functional. For this reason, calculations have also been performed using the BLYP and B3P86 functionals together with the aug-cc-pVDZ basis for the linear C_5^- cluster. In both cases, two imaginary vibrational modes are still observed (502i, 360i, and 404i; 169i cm^{-1}, respectively). In the second step, calculations have been performed using the B3LYP functional combined with the cc-pVDZ basis set. The final result is a linear structure ($D_{\infty h}$) as the most stable form (1.293, 1.327 Å; 163, 167, 359, 434, 656, 777, 787, 1472, 1900, 1923 cm^{-1}). A similar observation can be made for the linear isomer of C_{10}^-. In this case, from ROHF/DZP calculations,Watts et al.[24] and Schmatz et al.[29] predict a linear and centrosymmetric structure with a $^2\Pi_u$ ground state, whereas our B3LYP/aug-cc-pVDZ geometry optimizations lead to a bent structure of C_2 symmetry with a ^2A ground state. At the latter level, the linear structure lies 0.31 kcal mol^{-1} above the bent geometry and is characterized by four highly significant imaginary frequencies (1086i, 1065i, 618i, 617i cm^{-1}). Here also, when C_{10}^- is optimized at the B3LYP/cc-pVDZ level, the linear structure ($D_{\infty h}$) is predicted to be the ground-state minimum form (1.281, 1.327, 1.263, 1.319, 1.263 Å; 45, 46, 117, 119, 213, 218, 297, 307, 410, 418, 431, 541, 562, 681, 711, 780, 792, 818, 1150, 1476, 1900, 1997, 2099, 2167, 2204 cm^{-1}). Because the ground state of the linear C_n^- anions is $^2\Pi$, these species are expected to exhibit Renner−Teller splitting.[66,67] When the Renner−Teller effect is small, the molecular species will remain linear.[68] The peculiar behavior of the C_n^- ($n = 5,7-10$) clusters can therefore be ascribed to a "strong"[68] Renner−Teller effect at the B3LYP/aug-cc-pVDZ level.

Diffuse *d* basis functions appear to be responsible for the slight torsion of most carbon anion chains (C_5^-, C_7^-, C_8^-, C_9^-, C_{10}^-) in low-symmetry (C_s, C_2, C_{2v}, C_2, and C_2, respectively) structures. To assess this point, the geometries of these species have been reoptimized using the B3LYP approach and the cc-pVDZ basis set augmented by a set of {s} or {sp} diffuse functions (in short, cc-pVDZ+{s} and cc-pVDZ+{sp}, respectively) taken from the aug-cc-pVDZ basis set. At these levels, all carbon anion chains appear to be strictly linear and centrosymmetric. It must be further noted that all geometry optimizations reported so far for carbon anion chains larger than C_4^- were performed either under the "natural assumption" (i.e., constraint) of a $D_{\infty h}$ point group[24,27−29] or by using basis sets that did not incorporate *d* diffuse functions.[27−30,35,39,41] The most thorough available investigations of the molecular structure of the linear isomers of C_3^- and C_4^- are based on CCSD(T) calculations using basis sets of 255 or 256 contracted Gaussian-type orbitals, among which is a set of *s*, *p*, and *d* diffuse functions (see ref 29 and references therein for details). These calculations show unequivocally[29] that these anion species are strictly linear and centrosymmetric, which further strengthens our confidence in B3LYP/aug-cc-pVDZ structural investigations on C_n^- clusters (at the latter level, the $D_{\infty h}$ point group also prevails for the C_3^- and C_4^- chains).

Further ab initio calculations confirm the Renner−Teller distortion of the molecular structures of the C_5^-, C_7^-, C_8^-, C_9^-, and C_{10}^- chains due to the double energy degeneracy of their electronic ground state in a $D_{\infty h}$ configuration. Geometry reoptimization, at the MBPT(2)/aug-cc-pVDZ level, of the obtained B3LYP/aug-cc-pVDZ structures indicates comparable or even stronger distortions from linearity than those reported in Table 1 (C_5^-: $\theta_{123} = 176.49°$, $\theta_{234} = 173.75°$; C_7^-: $\theta_{123} = 179.46°$, $\theta_{234} = 179.70°$, $\theta_{345} = 179.59°$,; C_8^-: $\theta_{123} = 178.34°$, $\theta_{234} = 177.20°$, $\theta_{345} = 177.76°$; C_9^-: $\theta_{123} = 177.08°$, $\theta_{234} = 177.33°$, $\theta_{345} = 176.71°$, $\theta_{456} = 179.92°$; C_{10}^-: $\theta_{123} = 175.49°$, $\theta_{234} = 177.31°$, $\theta_{345} = 176.97°$, $\theta_{456} = 178.37°$). The obtained MBPT(2)/aug-cc-pVDZ energy differences between the linear and centrosymmetric ($D_{\infty h}$) saddle forms and the bent energy-minimum forms of the linear isomers of C_5^-, C_7^-, C_8^-, C_9^-, and C_{10}^- are 0.25, 0.04, 0.11, 0.80, and 0.46 kcal mol^{-1}, respectively. These energy differences are in line with the results of more reliable single-point CCSD(T)/aug-cc-pVDZ calculations on the geometries optimized for these anion species at the B3LYP/aug-cc-pVDZ level. In the same order, these indicate that the $D_{\infty h}$ configurations are less stable than the bent structures by 0.25, 0.16, 0.33, 0.87, and 0.83 kcal mol^{-1}. Notice that at the MBPT(2)/aug-cc-pVDZ level and under the constraint of $D_{\infty h}$ symmetry the C_4^- and C_6^- chains do not show any imaginary vibrational frequencies, which further confirms the linearity of these species.

3.2. Rotational Moments of the Linear Clusters. As shown in our previous study of carbon cations,[59] rotational spectroscopy can provide useful and very sensitive insights into the complex

TABLE 3: Total Lengths[a] (Å) and Moments of Inertia[b] (kg m²) of Linear Carbon Clusters in Their Neutral and Negatively Charged Forms

species		total length	moments of inertia I_{xx} ($\times 10^{-46}$)	I_{yy} ($\times 10^{-46}$)	I_{zz} ($\times 10^{-46}$)
Even-Membered Species					
C_4	($D_{\infty h}$)	3.936	0.000	17.112	17.112
C_4^-	($D_{\infty h}$)	3.913	0.000	17.055	17.055
C_6	($D_{\infty h}$)	6.494	0.000	58.608	58.608
C_6^-	($D_{\infty h}$)	6.488	0.000	58.860	58.860
C_8	($D_{\infty h}$)	9.057	0.000	139.566	139.566
C_8^-	(C_{2v})	9.059	0.005	140.176	140.183
C_{10}	($D_{\infty h}$)	11.624	0.000	273.364	273.364
C_{10}^-	(C_2)	11.629	0.008	274.158	274.160
Odd-Membered Species					
C_3	($D_{\infty h}$)	2.602	0.000	6.745	6.745
C_3^-	($D_{\infty h}$)	2.630	0.000	6.890	6.890
C_5	($D_{\infty h}$)	5.174	0.000	33.314	33.314
C_5^-	(C_s)	5.202	0.005	33.746	33.751
C_7	($D_{\infty h}$)	7.744	0.000	92.753	92.753
C_7^-	(C_2)	7.772	0.005	93.648	93.649
C_9	($D_{\infty h}$)	10.315	0.000	198.245	198.245
C_9^-	(C_2)	10.341	0.010	199.530	199.532

[a] Obtained by summing the bond lengths. [b] Moments of inertia of the structures optimized at the B3LYP/aug-cc-pVDZ level. Atomic units have been converted into SI units using $[L] = a_0 = 5.2917 \times 10^{-11}$ m; $[M] =$ amu $= 1.6605 \times 10^{-27}$ kg.

structural variations induced by an adiabatic ionization process or, similarly, by an adiabatic electron-attachment event. The moments of inertia of the investigated C_n^- chains and of their neutral counterparts are presented in Table 3. Upon analysis of the structural parameters, also reported in this Table, it is immediately noticeable that adiabatic electron-attachment processes nearly systematically yield an increase in the length of the chains, which in turn induces an increase in the moments of inertia. For the even-membered clusters, the increase in length is the result of a rather global structural alteration (Tables 1 and 3), whereas for the odd-membered species, the major structural alterations are principally observed at the extremities of the chain.

Two exceptions to this behavior arise for C_4 and C_6. In the latter case, the total length of the chain is slightly decreased in the anion form. Despite this, electron attachment induces an increase in the moments of inertia except for C_4.

3.3. Structural and Topological Properties of Cyclic Clusters. Most anionic structures of cyclic carbon clusters optimized in this work appear to be strictly planar, the exceptions being the C_5^-, C_8^-, C_9^-, and C_{13}^- rings. The bond lengths for the cyclic anions C_n^- with $n = 4-13$ are collected in Table 4. For comparison purposes and in order to evaluate the impact of adding one extra electron to the neutral species, the bond lengths of the neutral clusters in their singlet ground states are also included in this Table. To simplify the comparison of the neutral and anion structures, we further quantify (Table 5) the bond-length alternations in both series by taking the absolute value of the differences between successive bond lengths.

In contrast to our previous analysis for the neutral C_n and the cation C_n^+ clusters,[58,59] we find that it is not easy to determine whether C_n^- rings have polyynic[69] or cumulenic[58] character. C_8^- and C_{12}^- are derived from polyynic neutral forms,[59] but in comparison with their neutral counterparts, they display a reduced alternation of bond lengths, which implies stronger cumulenic character. C_8^- is particularly attractive

TABLE 4: Geometries of the Cyclic C_n^- ($n = 4-13$) Anions at the B3LYP/aug-cc-pVDZ Level

C_4^-	
$^2B_{2g}$ (D_{2h})	$r = 1.462$
$^2B_{2g}$ (D_{2h}) SDQ-MBPT(4)[a]	$r = 1.460$
$^2B_{2g}$ (D_{2h}) MBPT(2)[b]	$r = 1.488$
^1A_g (D_{2h}) neutral[c]	$r = 1.454$
C_5^-	
$^2A_1$ (C_2)	$r_{21} = 1.399$, $r_{32} = 1.451$, $r_{43} = 1.517$
$^1A_1$ (C_2) neutral[c]	$r_{21} = 1.365$, $r_{32} = 1.436$, $r_{43} = 1.568$
C_6^-	
$^2A'_1$ (D_{3h})	$r = 1.367$
$^1A'_1$ (D_{3h}) neutral[c]	$r = 1.332$
C_7^-	
$^2B_2$ (C_{2v})	$r_{21} = 1.411$, $r_{32} = 1.338$, $r_{43} = 1.344$, $r_{54} = 1.428$
$^2B_1$ (C_{2v}) ROHF[d]	$r_{21} = 1.349$, $r_{32} = 1.309$, $r_{43} = 1.485$, $r_{54} = 1.261$
$^1A_1$ (C_{2v}) neutral[c]	$r_{21} = 1.332$, $r_{32} = 1.352$, $r_{43} = 1.405$, $r_{54} = 1.270$
C_8^-	
$^2A_2$ (D_{2d})	$r = 1.339$
^1A_g (C_{4h}) neutral[c]	$r_{21} = 1.267$, $r_{32} = 1.389$
C_9^-	
^2A (C_2)	$r_{21} = 1.315$, $r_{32} = 1.323$, $r_{43} = 1.309$, $r_{54} = 1.284$, $r_{65} = 1.350$
^1A (C_2) neutral	$r_{21} = 1.314$, $r_{32} = 1.320$, $r_{43} = 1.311$, $r_{54} = 1.312$, $r_{65} = 1.335$
C_{10}^-	
$^2A_1$ (C_{2v})	$r_{21} = 1.355$, $r_{32} = 1.269$, $r_{43} = 1.337$, $r_{54} = 1.293$, $r_{65} = 1.321$
$^1A'_1$ (D_{5h}) neutral[c]	$r = 1.301$
C_{11}^-	
$^2A_2$ (C_{2v})	$r_{21} = 1.307$, $r_{32} = 1.339$, $r_{43} = 1.279$, $r_{54} = 1.380$, $r_{65} = 1.243$, $r_{76} = 1.397$
$^2A_2$ (C_{2v}) B3LYP[e]	$r_{21} = 1.304$, $r_{32} = 1.336$, $r_{43} = 1.277$, $r_{54} = 1.378$, $r_{65} = 1.241$, $r_{76} = 1.403$
$^1A_1$ (C_{2v}) neutral[c]	$r_{21} = 1.303$, $r_{32} = 1.321$, $r_{43} = 1.286$, $r_{54} = 1.351$, $r_{65} = 1.255$, $r_{76} = 1.367$
C_{12}^-	
^{2}? (C_{6h})	$r_{21} = 1.284$, $r_{32} = 1.332$
^{1}? (C_{6h}) neutral[c]	$r_{21} = 1.255$, $r_{32} = 1.357$
C_{13}^-	
^2A (C_2)	$r_{21} = 1.301$, $r_{32} = 1.300$, $r_{43} = 1.301$, $r_{54} = 1.299$, $r_{65} = 1.298$, $r_{76} = 1.299$, $r_{87} = 1.296$
$^1A_1$ (C_{2v}) neutral[c]	$r_{21} = 1.301$, $r_{32} = 1.285$, $r_{43} = 1.315$, $r_{54} = 1.271$, $r_{65} = 1.325$, $r_{76} = 1.262$, $r_{87} = 1.328$

[a] Reference 37. [b] Reference 38. [c] Reference 58. [d] Reference 32. [e] Reference 34.

because the bond lengths of this nonplanar (D_{2d}) structure are equal, in sharp contrast to the planar (C_{4h}) neutral C_8 ring. Conversely, the planar, cumulenic nature of C_6 is entirely preserved in its anion form, whereas C_{10}^- shows a stronger bond-length alternation. This contrasted behavior can be explained only by the topologies and degeneracies of the frontier orbitals, namely, the highest occupied and lowest unoccupied molecular orbitals (HOMO and LUMO, respectively).

The C_8 ring is a planar cluster that displays two nondegenerate orbitals of π symmetry with different phases as HOMO and LUMO (Figure 1). As is usually the case, the topology of the HOMO (in this case, $1b_u$) dictates the bond orders in the neutral

TABLE 5: Successive Bond-Length Alternations (Å) in Cyclic Carbon Clusters in Their Ground States

C_4^+	0.000								
C_4^-	0.000								
C_4	0.000								
					$4n$ Species (Polyynic Neutrals)				
C_8^+	0.062								
C_8^-	0.000								
C_8	0.123								
C_{12}^+	0.052								
C_{12}^-	0.048								
C_{12}	0.102								
					$4n + 2$ Species (Cumulenic Neutrals)				
C_6^+	0.032	0.059	0.000						
C_6^-	0.000	0.000	0.000						
C_6	0.000	0.000	0.000						
C_{10}^+	0.018	0.030	0.029	0.016					
C_{10}^-	0.086	0.068	0.044	0.028					
C_{10}	0.000	0.000	0.000	0.000					
					$4n + 1$ Species (Cumulenic Neutrals)				
C_5^+	0.168	0.045	0.049	0.174	0.002				
C_5^-	0.052	0.066	0.066	0.052	0.000				
C_5	0.071	0.132	0.132	0.071	0.000				
C_9^+	0.041	0.077	0.105	0.117	0.117	0.105	0.077	0.041	0.000
C_9^-	0.008	0.015	0.042	0.066	0.066	0.042	0.015	0.008	0.000
C_9	0.003	0.009	0.008	0.023	0.023	0.008	0.009	0.003	0.000
C_{13}^+	0.033	0.057	0.077	0.093	0.104	0.104			
C_{13}^-	0.0005	0.0004	0.001	0.001	0.0001	0.003			
C_{13}	0.016	0.030	0.044	0.053	0.062	0.065			
					$4n + 3$ Species (Polyynic Neutrals)				
C_7^+	0.0001	0.002	0.001	0.079	0.079	0.001	0.002		
C_7^-	0.074	0.006	0.084	0.084	0.006	0.074	0.000		
C_7	0.020	0.053	0.135	0.135	0.053	0.020	0.000		
C_{11}^+	0.008	0.018	0.030	0.044	0.057				
C_{11}^-	0.031	0.060	0.101	0.137	0.153				
C_{11}	0.018	0.036	0.065	0.096	0.011				

form (i.e., the bonding overlaps in the HOMO fall at the same location as the "triple" bonds in this cyclic species, whereas the "single" bonds are easily recognizable from the antibonding overlaps). The orbital below the HOMO (HOMO-1) in the C_8 ring, $5b_g$, is a nondegenerate orbital of σ symmetry with bonding and antibonding patterns similar to those seen in the HOMO, which justifies the polyynic depiction of this cluster. However, for the LUMO, $2b_u$, the bonding overlaps are located on the single bonds, whereas the triple bonds are associated with antibonding overlaps. Because of the phase relationships (Figure 1) that prevail between the HOMO and the LUMO, an electron-attachment process on the LUMO ($2b_u$) of the C_8 ring obviously implies a shortening of the single bonds and an extension of the triple bonds. The same observations apply to the next polyynic ring, C_{12}. The further distortion from planarity seen in C_8^- is the outcome of a pseudo-Jahn−Teller effect, which releases a near-degeneracy in energy with the LUMO+1 orbital ($6a_g$) in the neutral form and enables a stronger localization of the extra electron (Figure 1).

The case of the smallest cumulenic system, the C_6 ring, is easier to treat and is analyzed in Figure 2. The four outermost occupied levels of C_6 belong to two sets (HOMO: 1e″, HOMO-1: 5e′) of doubly degenerate orbitals of π and σ symmetry. In line with the cumulenic (doubly aromatic) nature of this cyclic cluster, these belong to the out-of-plane and in-plane "π" conjugation band systems, respectively. The LUMO ($5a'_1$), on the contrary, is a nondegenerate, well-isolated, fully symmetric orbital. Filling this orbital with an electron, therefore, cannot lead to any major structural alteration. In turn, this orbital remains almost unchanged when it becomes the singly occupied molecular orbital (SOMO) of the C_6^- species. However, for the next cumulenic ring, C_{10}, the LUMO ($2e''_2$) has double energy degeneracy. In this case, an electron attachment also gives rise to a pronounced Jahn−Teller effect in the form of a lowering of the symmetry point group from D_{5h} to C_{2v}, which explains the rather strong bond-length alternation of the anionic form.

The trends for the odd-membered cyclic carbon clusters are even more complicated. An earlier work[59] on the structural distortions induced by an adiabatic ionization process has shown that the members of the C_{4n+1} ($n = 1-4$) series could be consistently classified as "cumulenic" species, whereas the C_{4n+3} rings should rather be described as "polyynic" systems. As emphasized above for C_6, C_8, and C_{10}, this partition is related only to the topology of the *highest* occupied orbitals in the σ- and π-band systems and to their impact on bond order. It can certainly not be used to determine the behavior of these clusters upon adiabatic electron attachment, which exclusively depends on the topology and energy degeneracies (or near-energy degeneracies) of the lowest unoccupied orbitals. For instance, in line with our previous observations regarding C_8 and C_6, an adiabatic electron-attachment process on the polyynic C_7 ring yields an overall substantial reduction of the bond-length alternation, making the structure more cumulenic, whereas the opposite is observed for the cumulenic C_9 cyclic species. At odds with this behavior, a significant increase of the alternation of bond lengths is seen upon electron attachment on C_{11}, a species with strong polyynic character, and a reduction is seen with C_5 and C_{13}.

The members of the C_{4n+1} series are particularly exquisite structures to investigate. In their neutral form, the first two members (C_5, C_9) of this series show an inherent propensity for torsions of the π chemical bonds along the carbon backbone, resulting, in turn, in pronounced out-of-plane distortions of the molecular geometry into low-symmetry (C_2) structures. These torsions can be related[70] to the gerade symmetry of the HOMO of the linear counterparts, implying that an out-of-phase relationship prevails between the extremities of the chain. The departure from planarity enables enhanced orbital mixing in the form of a conjugative pattern of through-space bonding overlaps. As a result, the frontier orbitals (HOMO, LUMO) of these two species consist[70] of two intertwined tori winding around the carbon backbone. However, despite the gerade symmetry of the HOMO ($3\pi_g$) of the C_{13} cumulenic chain, the cyclic isomer of this species remains planar, owing to lesser cyclic strains.

In the present work, it has been found that besides enforcing the peculiar topology of the C_5 and C_9 rings, electron attachment also induces significant changes in the electronic structure of the next member of this series, C_{13} (a planar C_{2v} ring in its neutral form), through striking geometrical relaxation in a nonplanar C_2 structure (~0.07 Å deviations from planarity). As for the C_5, C_7, C_8, C_9, and C_{10} chains, diffuse *d* functions are also essential for a consistent description of all geometrical implications of electron attachment on the C_{13} ring. Indeed, a planar structure of C_{2v} symmetry is obtained for the cyclic C_{13}^- species upon B3LYP/cc-pVDZ+{s} and B3LYP/cc-pVDZ+{sp} geometry optimizations. At the B3LYP/aug-cc-pVDZ level, such a C_{2v} form describes a second-order saddle point ($\omega_1 = 270i$ cm^{-1}, $\omega_2 = 554i$ cm^{-1}) 0.58 kcal mol^{-1} above the energy minimum of C_2 symmetry.

The SOMO of the C_5^-, C_9^-, and C_{13}^- rings is displayed in Figure 3 and compared with the lowest unoccupied molecular

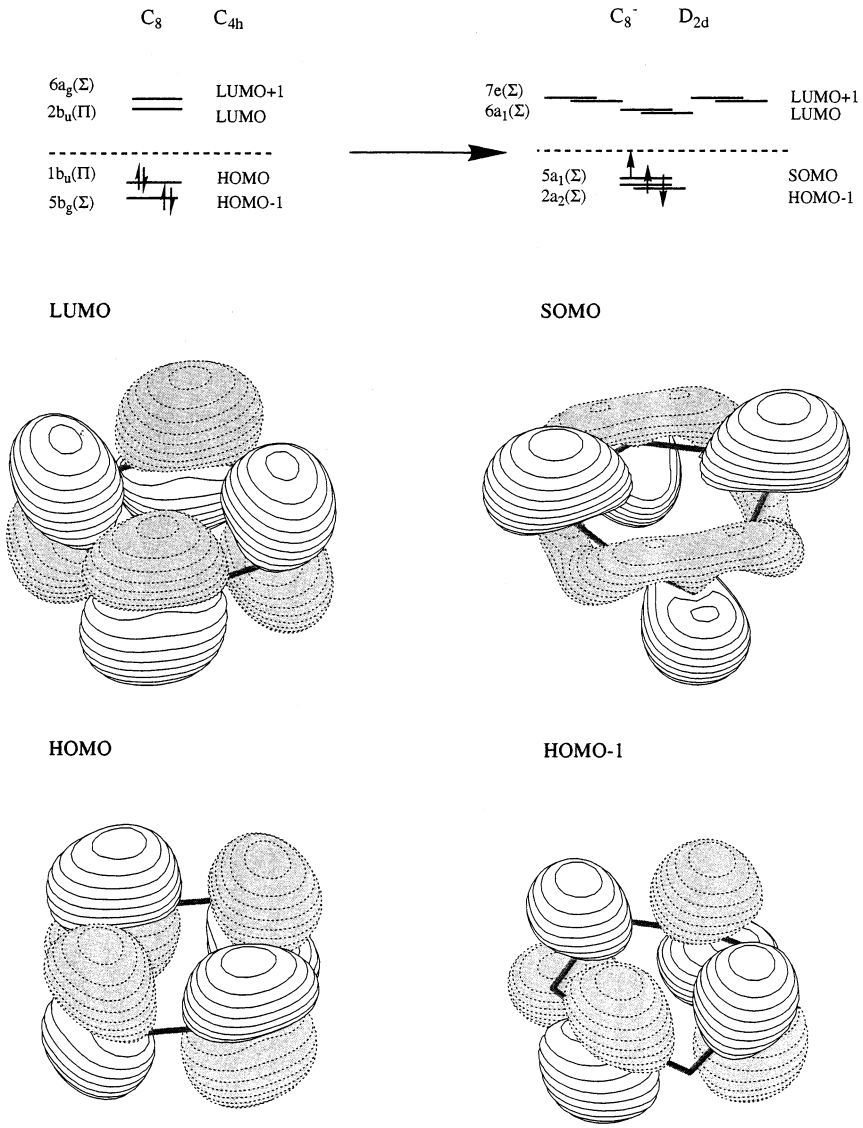

Figure 1. Energy diagram for the two outermost occupied orbitals of the C_8 and C_8^- cyclic clusters. Schematic drawings of the highest occupied molecular orbital (HOMO) and the lowest unoccupied molecular orbital (LUMO) of C_8 and of the singly occupied molecular orbital (SOMO) and the HOMO-1 of C_8^-.

orbitals of the neutral counterparts, for which planarity has been imposed in order to understand puzzling topological features of the frontier orbitals of these carbon rings. Notice that for C_5 and C_9 the C_{2v} forms are first-order or second-order saddle points connecting structurally equivalent structures of C_2 symmetry. Relative to the C_2 minimum-energy forms of the C_5 and C_9 rings, these stationary points are 54.14 and 4.94 kcal mol^{-1} higher in energy, respectively. The relationships between the two series of orbitals displayed in Figure 3 are very clear. The LUMOs of the neutral C_{2v} forms of the cyclic isomers of C_5, C_9, and C_{13} are nicely delocalized orbitals of σ symmetry that display one, two, and three radial nodal surfaces across the plane of the ring, respectively, as well as a circular nodal surface that closely follows the carbon backbone. This nodal structure can, in turn, be related to the topology of the corresponding LUMO orbitals ($2\pi_u$, $3\pi_u$, $4\pi_u$) in the linear isomer,[70] which shows one nodal plane along the chain as well as two, four, and six transversal nodal planes, respectively. The LUMO of the C_{2v} form of the C_5 and C_9 rings shows rather pronounced localization properties that are consistent with the unstable and strained nature of these planar saddle points, whereas the LUMO of the (geometrically stable) planar C_{13} ring is fully delocalized. In sharp contrast to the topology of the LUMO orbitals in the planar rings, the topology of the SOMOs of the C_5^-, C_9^- and C_{13}^- cyclic species in their C_2 global energy minimum consists of only one closed nodal surface winding around the ring, which separates two intertwined tori with opposite phases. This nodal surface and the tori are characterized by two, four, and six twists by 180°, respectively, which are clearly reminiscent of the phase inversions seen in the neutral and planar counterparts. For these reasons, the cyclic isomers of C_5^-, C_9^-, and C_{13}^- can be described as even-twisted cumulenic rings. The SOMOs of these three closed anionic clusters are perfectly delocalized and therefore strongly bonding orbitals. In line with the aromaticity rules for Hückel cycles,[71] particularly high electron affinities are therefore to be expected for the C_{4n+1} rings ($n = 1-3$).

3.4. Rotational Moments of the Cyclic Clusters. The moments of inertia and the circumferences of the neutral and anion clusters are displayed in Table 6. Upon inspection of the values reported in this table, it is clear that an electron-attachment process on the even-membered clusters systematically leads to a very significant increase in the component I_{zz} along the main symmetry axis, which reflects an increase in system size in comparison with that of the neutral counterparts.

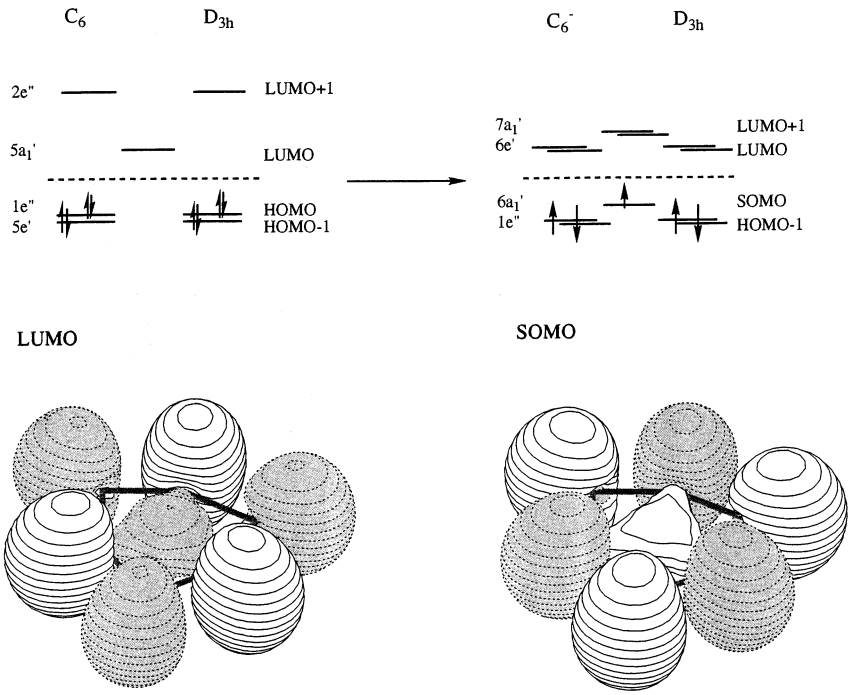

Figure 2. Energy diagram for the four outermost occupied orbitals of the C_6 and C_6^- cyclic clusters. Schematic drawings of the lowest unoccupied molecular orbitals (LUMO) and of the singly occupied molecular orbital (SOMO) of the neutral and the anionic species, respectively.

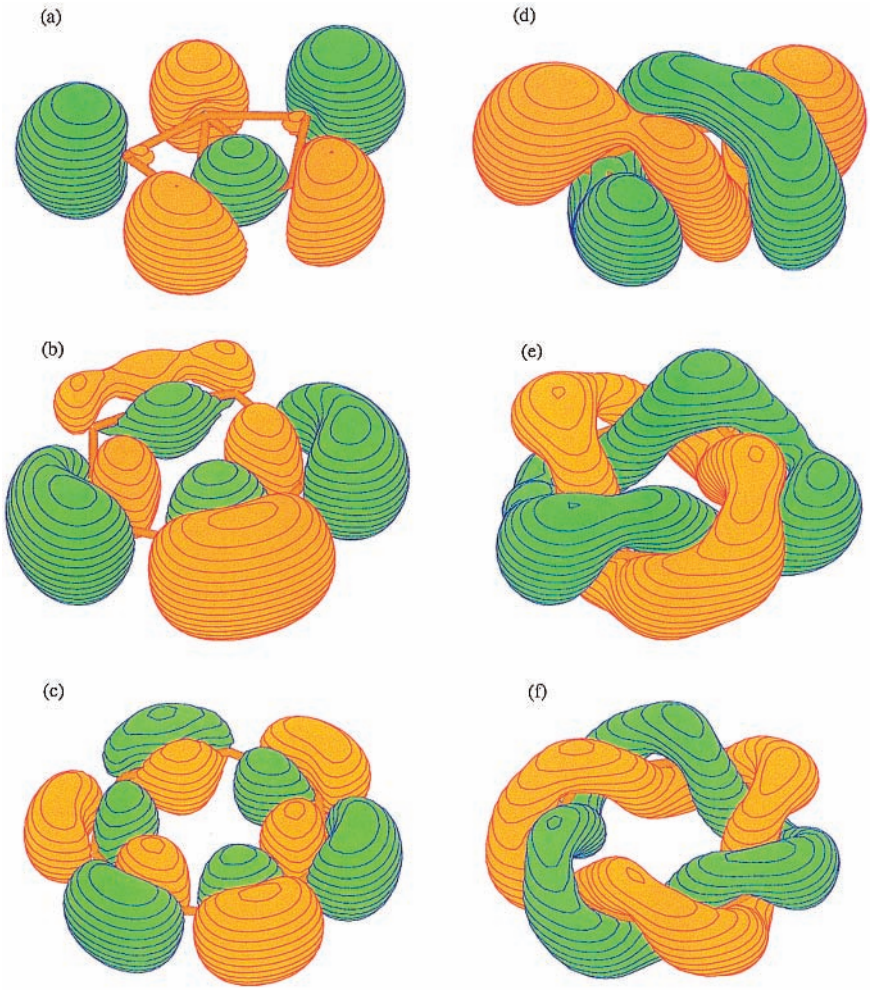

Figure 3. Lowest unoccupied molecular orbitals of the (a) C_5, (b) C_9, and (c) C_{13} clusters in planar configuration and singly occupied molecular orbitals of the (d) C_5^-, (e) C_9^-, and (f) C_{13}^- clusters in their global energy minimum forms (see text for further explanation).

TABLE 6: Total Circumference Values[a] (Å) and Moments of Inertia[b] (kg m^2) of Cyclic Carbon Clusters in Their Neutral and Negatively Charged Forms

species		total length	moments of inertia I_{xx} ($\times 10^{-46}$)	I_{yy} ($\times 10^{-46}$)	I_{zz} ($\times 10^{-46}$)
Even-Membered Species					
C_4	(D_{2h})	5.818	2.266	6.164	8.430
C_4^-	(D_{2h})	5.847	2.170	6.345	8.514
$4n$ Species (Polyynic Neutrals)					
C_8	(C_{4h})	10.624	22.826	22.826	45.652
C_8^-	(D_{2d})	10.710	22.838	22.838	44.372
C_{12}	(C_{6h})	15.673	74.055	74.055	148.110
C_{12}^-	(C_{6h})	15.698	74.126	74.126	148.251
$4n + 2$ Species (Cumulenic Neutrals)					
C_6	(D_{3h})	7.991	10.163	10.163	20.357
C_6^-	(D_{3h})	8.201	10.668	10.668	21.337
C_{10}	(D_{5h})	13.011	42.959	42.959	85.917
C_{10}^-	(C_{2v})	13.149	39.564	48.016	87.579
Odd-Membered Species					
$4n + 3$ Species (Polyynic Neutrals)					
C_7	(C_1)	9.447	12.670	19.068	31.738
C_7^-	(C_{2v})	9.613	11.775	20.834	32.610
C_{11}	(C_{2v})	13.031	56.102	58.179	114.281
C_{11}^-	(C_{2v})	14.494	56.303	59.362	115.665
$4n + 1$ Species (Cumulenic Neutrals)					
C_5	(C_2)	7.169	4.938	9.262	12.684
C_5^-	(C_2)	7.218	4.674	9.736	13.516
C_9	(C_1)	11.849	31.559	31.967	63.080
C_9^-	(C_2)	11.880	31.108	33.219	64.185
C_{13}	(C_{2v})	16.846	93.597	94.301	187.899
C_{13}^-	(C_2)	16.891	93.675	94.860	188.468

[a] Obtained by summing the bond lengths. [b] Moments of inertia of the structures were optimized at the B3LYP/aug-cc-pVDZ level. Atomic units have been converted into SI units using [L] = $a_0 = 5.2917 \times 10^{-11}$ m; [M] = amu = 1.6605×10^{-27} kg.

The sole exception to this behavior arises with C_8, for which a significant decrease of the main axis component is observed upon electron attachment despite an increase in the ring's circumference. Obviously, this anomaly relates to the strong departure from planarity that is seen with the C_8^- cyclic anion. Further inspection of the results displayed in Table 6 indicates that C_6 and C_{12} are symmetric tops in their neutral and anionic forms. The structural distortions that arise during electron attachment on C_{10}, a symmetric top in its neutral form, are easily recognizable from the asymmetry of the top that characterizes the C_{10}^- anion. Very generally, and rather unsurprisingly, the odd-membered clusters are found to be asymmetric rotors both in the neutral and anionic forms. For these clusters, the asymmetry of the top tends to increase upon adiabatic electron attachment, which reflects either the enforcement of the nonplanar nature of C_5 and C_9, the departure from planarity in the case of C_{13}^-, or the increased bond-length alternations of C_{10}^- and C_{11}^-.

3.5. Energy Considerations. The total energies of the cyclic and linear forms of carbon clusters at various theoretical levels (ROHF, B3LYP, CCSD(T)) are compared in Table 7. All data presented in this Table are the results of further single-point calculations using the optimized B3LYP/aug-cc-pVDZ geometries along with the aug-cc-pVDZ basis set. Absolute energies (in au) are listed for the most stable forms, whereas the relative energies of the less-stable isomers are expressed in kcal mol^{-1}. It appears that all theoretical levels, including ROHF, predict the same energy sequence. In the range of the C_n^- clusters that have been considered, ($n = 3-10$), the linear species are systematically the most stable structures. The aug-cc-pVDZ basis set leads to severe linear dependencies and convergence problems when applying the B3LYP approach, and for this reason, the B3LYP/aug-cc-pVDZ calculations on the linear anionic species larger than C_{10}^- had to be dropped. Rather fortunately, the dependence of the total energy on the size of these linear species is extremely regular (Figure 4), permitting a linear extrapolation to larger clusters. For the sake of comparison, we also display in this Figure the results of previous B3LYP/cc-pVDZ calculations[58,59] on neutral C_n and cation C_n^+ cyclic and linear isomers.

As is immediately apparent from Figure 4, the crossing point between the cyclic and linear series is at C_7^+ for the cations and at C_{10} for the neutral species, which is in line with the experimental observation.[32] By extrapolation of the energies calculated for the linear anionic species up to C_{10}^-, the crossing point seems to coincide with C_{13}^- for the anion, which is also in line with some experimental observations.[22] Notice, however, that the more reliable single-point CCSD(T)/aug-cc-pVDZ energies reported in Table 7 indicate that the linear and cyclic isomers of C_{10}^- are practically isoenergetic.

From a more detailed analysis of our single-point CCSD(T) data (see the last entry of Table 7), we notice that the so-called T_1 diagnostic[72,73] (Table 7) is always larger than 0.02, which reflects the importance of the nondynamical correlation effects in the ground state of the smaller C_n^- carbon clusters. Nonetheless, the T_1 diagnostic generally produces values much smaller than 0.08, which justifies[74] the description of the ground state by a single-determinant wave function.

3.6. Vibrational Spectra. The vibrational frequencies and related IR activities of all the carbon cluster anions that have been investigated are displayed in Table 8. The dependence of the IR activity of the most intense lines on system size is depicted in Figure 5[5] for the anionic species. As for the neutral species and the cations,[58,59] the linear carbon anions generally have much higher IR activity than the cyclic species. For the linear anions, the most intense lines have an IR activity ranging from 123 km mol^{-1} (C_4^-) to 5273 km mol^{-1} (C_9^-), whereas for the cyclic anions, the maximum in IR activity lies between 35 km mol^{-1} (C_4^-) and 1003 km mol^{-1} (C_{11}^-).

From Figure 5, it is clear that for the linear anions the IR activity increases rather regularly with the size of the chains, taking into account oscillations with a $2n$ periodicity. For the C_n^- chains, odd or even values of n correspond respectively to minima and maxima in the IR activity versus n plot. The intensities of the anions are comparable in magnitude with those of the cations but appear to be consistently smaller than those of the neutral chains. Conversely, as was previously noticed for the neutral species and cations,[58,59] the IR activity of the cyclic anions does not systematically increase with the size of the rings. Here also, a $4n$ periodicity is observed with the even-membered species: the C_{4n+2}^- systems coincide with a drop in IR activity, whereas the C_{4n}^- ($n = 2$ and 3) rings are characterized by a rise in intensity.

The size dependence and importance of IR activity that is associated with the asymmetric vibrational normal modes of linear C_n^+, C_n, and C_n^- chains is, as previously noted,[59] due to the presence of the two terminal carbon lone pairs, which results in large, size-extensive quadrupole moments. As for the cations and neutral carbon rings, the stronger IR activity of the polyynic cyclic species compared to that of the cumulenic species can be understood by considering the higher alternations of electric

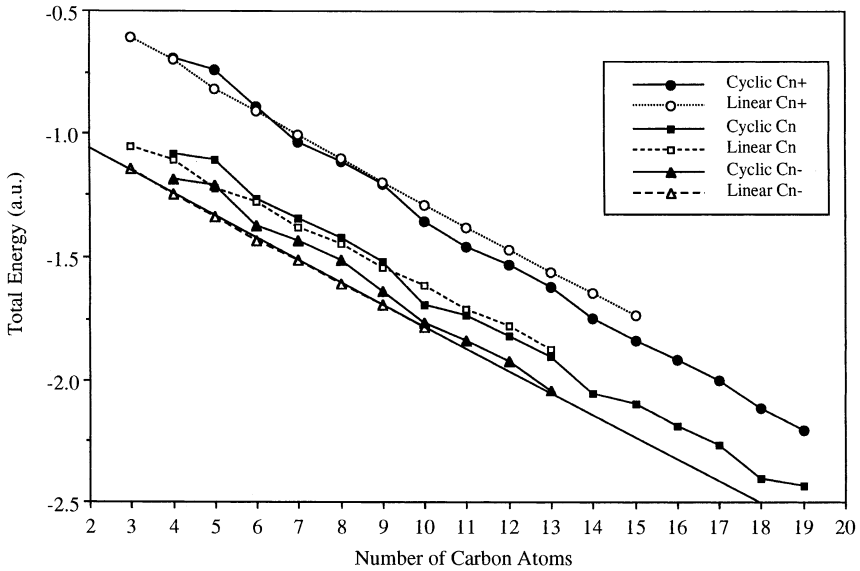

Figure 4. Size dependence of the total energy of the neutral, cationic, and anionic carbon cluster rings and chains.

TABLE 7: Total Energies (au) and Relative Energies (kcal mol^{-1}) of Isomers of C_n^- ($n = 3-13$) at Different Theoretical Levels (aug-cc-pVDZ basis set)

	ROHF	B3LYP	CCSD(T)	T_1 diagnostic
C_3^-				
linear doublet	−113.364478	−114.142747	−113.741553	0.028
C_4^-				
linear doublet	−151.281467	−152.188199	−151.819885	0.024
cyclic doublet	37.8	38.0	29.6	0.022
C_5^-				
linear doublet	−189.115324	−190.335413	−189.797292	0.030
cyclic doublet	84.3	78.8	67.4	0.047
C_6^-				
linear doublet	−226.969704	−228.431249	−227.783881	0.026
cyclic doublet	50.1	35.4	25.5	0.032
C_7^-				
linear doublet	−264.800454	−266.514914	−265.757934	0.031
cyclic doublet	66.3	49.7	37.6	0.024
C_8^-				
linear doublet	−302.651756	−304.607124	−303.741873	0.027
cyclic doublet		59.0	49.7	0.031
C_9^-				
linear doublet	−340.480744	−342.690107	−341.715186	0.032
cyclic doublet		32.1	24.6	0.037
C_{10}^-				
linear doublet		−380.780677	−379.697133	0.029
cyclic doublet		9.0	−0.06	0.038
C_{11}^-				
cyclic doublet		−418.836531		
C_{12}^-				
cyclic doublet		−456.924270		
C_{13}^-				
cyclic doublet		−495.044446		

charges on the atoms, leading to larger changes of the dipole moments upon distortion of the geometry during vibrations.

The IR spectra of C_n/C_n^- mixtures in argon and neon matrixes,[11−14,18] which have been measured from 1600−2200 cm^{-1}, have been extensively debated in a number of experimental studies.[11−14,18] Despite the fact that the computed harmonic frequencies might strongly differ from the experimental frequencies because of the anharmonicities and spectral shifts due to secondary interactions with the matrices, the bands seen in these spectra have been tentatively assigned on the basis of theoretical data obtained from B3LYP/6-31G* calculations on isolated clusters. The results obtained by Szczepanski et al.[11−14] at this level for linear anionic clusters from C_3^- and C_9^- are nicely corroborated by our calculations, which make use of a much larger and more reliable basis set (i.e., aug-cc-pVDZ). Furthermore, the assignment of the band observed by Freivogel et al.[18] at 2094.5 cm^{-1} in the neon matrix to the linear C_{10}^- species is also confirmed by our calculations in the form of a B3LYP/aug-cc-pVDZ vibrational line at 2196.0 cm^{-1} with particularly strong IR intensity (3205 km/mol).

Although our calculations show that cyclic anions larger than C_6^- possess IR-active bands at frequencies between 1600 and 2200 cm^{-1} (Table 8), the intensity of these bands is probably far too weak to permit identification of these species through IR measurements.

3.7. Adiabatic Electron Affinities. A large number of experimental studies[3,4] and ab initio calculations[23,24,26,34,36,38] of the vertical and adiabatic electron affinities of carbon clusters have been published. As a direct byproduct of our work, adiabatic electron affinities (AEAs) are also presented in Table 9. These are directly evaluated from the total energies obtained from the neutral and anionic structures at the B3LYP/aug-cc-pVDZ level, regardless of the zero-point vibrational energies (ZPE). A few test calculations showed that their impact on electron-attachment energies is less than 0.1 eV. Available experimental data are also included in Table 9, which overall compare very satisfactorily with our results and confirm the assignments of these data to linear species. For the sake of comparison, we also include in this Table the vertical electron-detachment energies (VEDEs) of carbon anions C_n^- as well as the vertical electron affinities (VEAs) of their neutral counterparts C_n. These binding energies were obtained as energy differences of the results of B3LYP/aug-cc-pVDZ single-point calculations on the C_n^- species using the geometry of the neutral cluster and on the C_n species using the geometry of the anion, respectively. The comparison of vertical and adiabatic electron affinities emphasizes particularly strong geometry relaxation effects on electron-attachment processes of several cyclic C_n species such as C_5, C_7, C_8, and C_{10}. Inspection of Table 9 also reveals very strong geometry relaxation effects, on the order of 1 eV, for electron-detachment processes from carbon anion rings such as C_7^- and C_{10}^-. For the remaining cyclic clusters as well

TABLE 8: Harmonic Frequencies (cm^{-1}) and IR Intensities (km mol^{-1}) of C_n^- Anions at the B3LYP/aug-cc-pVDZ Level[a]

C_3^-	
$D_{\infty h}$ linear doublet ZPE = 5.06	205(π_u, 30), 371(π_u, 7), **1769(σ_u, 213)**
C_4^-	
$D_{\infty h}$ linear doublet ZPE = 8.35	192(π_u, 41), 217(π_u, 15), **1768(σ_u, 123)**
D_{2h} cyclic doublet ZPE = 6.60	**492(b_{2u}, 35)**, 506(b_{3u}, 27), 1204(b_{1u}, 7)
C_5^-	
C_s linear doublet ZPE = 10.57	143(a′, 21), 164(a″, 18), 1463(a′, 30), **1893(a′, 1105)**, 1914(a′, 1)
C_2 cyclic doublet ZPE = 9.36	228(b, 18), 348(a, 31), 601(b, 1), **651(b, 181)**, 678(a, 1), 846(a, 1), 1459(b, 21)
C_6^-	
$D_{\infty h}$ linear doublet ZPE = 14.61	105(23), 110(21), 285(4), **2026(σ_u, 905)**
D_{3h} cyclic doublet ZPE = 15.20	406(a_2″, 4), 584(e′, 4), 922(e′, 75), **1600(e′, 374)**
C_7^-	
C_2 linear doublet ZPE = 16.33	75(a,22), 89(b,11), 222(a,5), 323(b,3), 535(a,8), 1082(b, 9), **1824(b, 2902)**, 1983(b, 233)
C_{2v} cyclic doublet ZPE = 17.62	209(b_2, 57), 214(b_1, 35), 488(b_2, 57), 499(a_1, 1), 501(b_1, 1), 608(a_1, 3), 738(b_2, 99), 988(a_1, 2), 1153(a_1, 1), **1301(b_2, 199)**, 1392(a_1, 65), 1605(b_2, 9), 1706(a_1, 8)
C_8^-	
C_{2v} linear doublet ZPE = 20.13	65(a_1,17), 110(b_1,21), 202,(b_1,10), 253(a_1,4), 484(a_1,1), 531(a_1,1), 958(b_2, 19), 1864(b_2, 644), **2166(b_2, 1920)**
D_{2d} cyclic doublet ZPE = 20.28	130(e, 54), 150(b_2, 2), 575(e, 63), 1051(e, 65), **1687(e, 873)**, 1729(b_2, 40)
C_9^-	
C_2 linear doublet ZPE = 22.89	45(b, 112), 51(a, 15), 133(b, 1), 190(8), 207(7), 327(b, 1), 497(b, 1), 560(b, 1), 872(b, 37), 1656(b, 880), **1805(b, 5273)**, 2078(b, 249)
C_2 cyclic doublet ZPE = 23.51	166(b, 1), 181(a, 5), 344(b, 32), 348(a, 1), 367(a, 14), 494(a, 50), 545(b, 56), 593(a, 4), 860(a, 19), 1050(a, 119), 1092(b, 136), 1373(b, 149), 1480(b, 76), 1838(b, 217), **1859(a, 406)**
C_{10}^-	
C_2 linear doublet ZPE = 26.71	42(a, 14), 62(b, 12), 116(b, 1), 149(b, 9), 179(a, 14), 221(b, 1), 245(a, 1), 462(a, 1), 632(b, 7), 717(a, 1), 791(b, 39), 1470(b, 40), 1987(b, 2045), **2196(b, 3205)**
C_{2v} cyclic doublet ZPE = 27.93	157(3), 205(b_1, 3), 297(6), 339(6), 362(55), 383(2), 404(b_1,1) 460(b_2, 56), 561(a_1, 33), 806(a_1, 3), 943(b_2, 80), 1037(a_1, 110), 1412(a_1, 8), 1520(b_2, 35), 1684(b_2, 12), 1924(a_1, 204), **1793(b_2, 297)**, 2098(a_1, 249)
C_{11}^-	
C_{2v} cyclic doublet ZPE = 29.90	50(b_2, 6), 93(a_1, 3), 126(2), 263(b_2, 15), 351(b_1, 11), 376(b_1, 15), 383(b_1, 2), 399(a_1, 103), 490(a_1, 96), 502(b_2, 186), 776(a_1, 10), 921(a_1, 66), 932(b_2, 69), 1265(a_1, 10), 1270(b_2, 5), **1481(b_2, 1003)**, 1513(a_1, 2), 1896(b_2, 35), 1929(a_1, 590), 2064(b_2, 138), 2118(a_1, 68)
C_{12}^-	
C_{6h} cyclic doublet ZPE = 33.03	137(1), 530(111 × 2), 897(137 × 2), **1867(891 × 2)**
C_{13}^-	
C_2 cyclic doublet ZPE = 35.47	111(b, 7), 147(b, 2), 323(a, 8), 370(a, 2), 398(a, 1), 415(a, 11), 435(a, 8), 437(b, 4), 459(a, 34), 461(a, 37), 846(a, 112), 850(b, 137), 1107(b, 289), 1583(a, 1), 1945(b, 27), 1953(a, 1), **2035(a, 311)**, 2036(a, 305)

[a] Only IR-active modes with intensity ≥1 km mol^{-1} are given. The most intense harmonic frequencies are displayed in bold. The zero-point energies (ZPE) are expressed in kcal mol^{-1}.

as for the carbon chains in general, the computed VEAs, AEAs, and VEDEs are overall very similar.

Rather unsurprisingly, therefore, the agreement between these values and the available experimental binding energies is particularly good for carbon chains. On average, the discrepancy between the calculated and observed VEDEs is less than 0.07 eV. When considering the AEAs, we found that the average discrepancy is around 0.12 eV. It is worth noting that the onset of the photoionization spectrum of C_n^- chains is very generally defined by a sharp 0−0 vibrational transition, enabling a straightforward evaluation of the lowest electron-detachment energies of these species. For the linear species, our results are found to sustain very nicely the comparison with AEAs calculated at other levels of theory[23−26,38,40−42]. In particular, Table 9 enables a comparison with a few AEAs obtained at the CCSD(T) level of theory.[24,26] Incidentally, for the larger chains (C_6-C_9), our AEA results at the B3LYP/aug-cc-pVDZ level compare better with the experimental values than do the CCSD-(T)/DZP+sp//ROHF/DZP results. This is probably related to the better quality of the geometries and basis sets that have been used in our calculations and certainly does not call into question the inherent superiority of the CCSD(T) scheme. For the smaller chains (C_3-C_5), the comparison between the B3LYP/aug-cc-pVDZ and best CCSD(T)/PVTZ+//ROHF/DZP adiabatic elec-

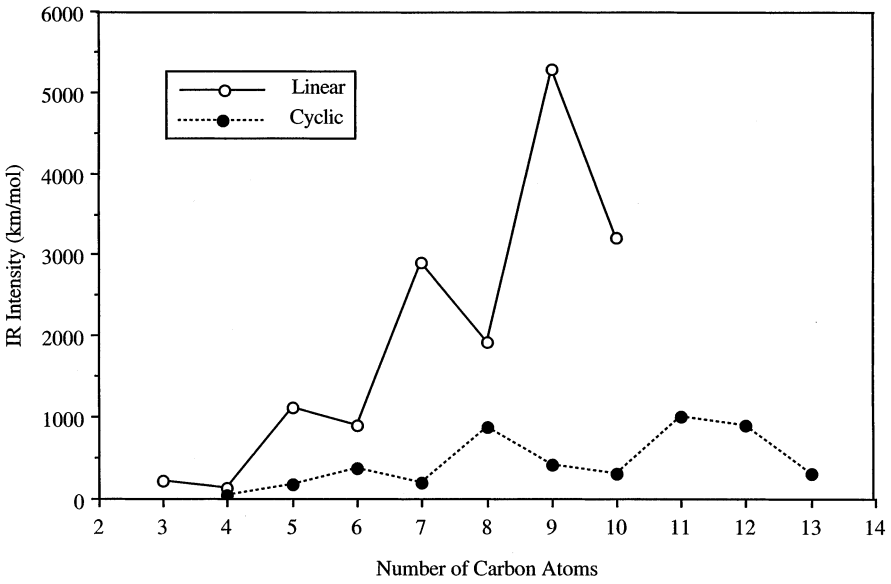

Figure 5. IR activity associated with the most intense line of linear and cyclic carbon clusters.

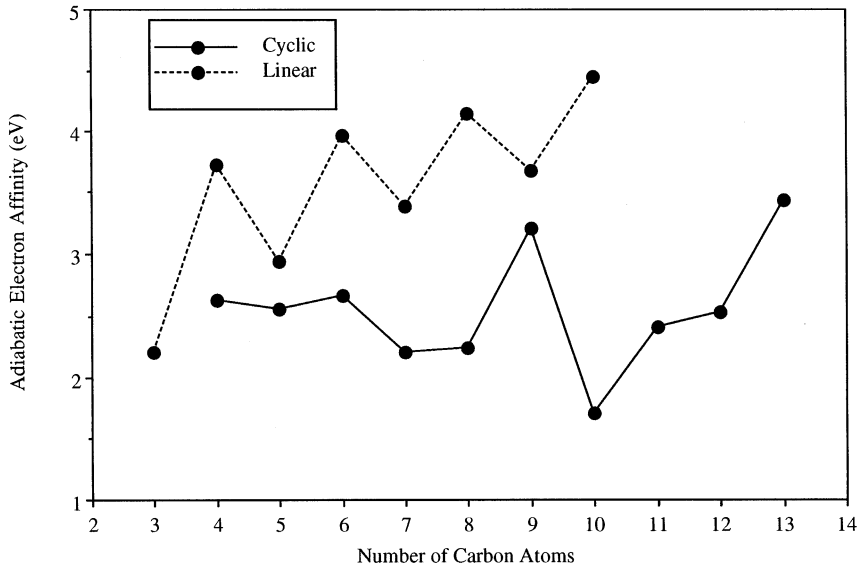

Figure 6. Size dependence of the adiabatic electron affinities of linear and cyclic C_n clusters.

tron affinities ultimately justifies the use of the DFT(B3LYP) approach in evaluating the electron affinities of larger carbon chains or rings.

With regard to the outcome of geometry relaxation effects on electron-attachment energies, much more care is required when comparing our results with the few experimental data available for the C_4^-, C_{10}^-, and C_{11}^- rings. The electron-detachment energy (2.2 eV) measured from anion photoelectron spectroscopy for the cyclic isomer of C_{10}^- lies between our AEA and VEDE estimates of 1.7 and 2.7 eV, respectively, which may indicate partial relaxation of the molecular geometry. Compared with our VEA, AEA, and VEDE results for the C_{11} ring, which very consistently indicate a binding energy of 2.4 $\pm$ 0.1 eV, the experimental value of 1.5$\pm$ 0.1 eV that is found for the ionization threshold of the C_{11}^- ring seems very doubtful. At this stage, it is worth mentioning that the latter two experimental values are apparently derived from a tricky extrapolation of the onset of ionization of C_{10}^- and C_{11}^- to the baseline of the spectrum.[5] Clearly, further measurements are required to clarify this issue experimentally.

As discussed previously for the C_8 chain, improving the basis set by inclusion of diffuse functions has a generally substantial impact on the calculated AEAs. A similar observation can be made for the linear C_5 and C_{10} clusters. The AEA value of 2.94 eV obtained at the B3LYP/aug-cc-pVDZ level reduces to 2.61 eV at the B3LYP/cc-pVDZ level for the linear isomer of C_5. These results must be compared with the experimental value of 2.839 $\pm$ 0.008 eV. Also, for the linear C_{10} cluster, an AEA value of 4.45 eV has been found when the aug-cc-pVDZ basis set has been used; this value reduces to 4.05 eV with the cc-pVDZ basis set. In the latter case, no experimental value is available.

As is immediately apparent from Figure 6, the AEAs of carbon clusters tend to increase overall with system size. As for the IR activities, the AEAs of the linear species follow a 2n periodicity, and the C_{2n} ($n = 2-5$) chains have systematically higher AEAs than do the C_{2n+1} ($n = 1-4$) chains. Among all of the investigated C_n rings ($n = 4-13$), by far the highest AEA values are observed for the C_9 and C_{13} species, which immediately reflects the very peculiar topological properties of

TABLE 9: Adiabatic Electron Affinities (AEA, eV) and Vertical Electron Affinities (VEA, eV) of Carbon Clusters C_n and Vertical Electron Detachment Energies (VEDE, eV) from Their Corresponding Anions C_n^-

species	B3LYP/aug-cc-pVDZ VEA	B3LYP/aug-cc-pVDZ AEA	B3LYP/aug-cc-pVDZ VEDE	CCSD(T) AEA	experimental values
C_3 linear	2.20	2.21	2.22	1.53[a]	1.981 ± 0.020[f]
				1.96[b]	1.995 ± 0.025[g]
					2.02 ± 0.03[h]
C_4 linear	3.56	3.72	3.85	3.52[a]	3.882 ± 0.010[g]
				3.85[b]	3.79 ± 0.01[h]
C_4 cyclic	2.60	2.63	2.65		2.1 ± 0.1[i]
C_5 linear	2.91	2.94	2.97	2.49[a]	2.839 ± 0.008[g]
				2.76[b]	2.83 ± 0.1[h]
C_5 cyclic	2.16	2.56	2.94		
C_6 linear	3.83	3.97	4.11	3.87[a]	4.185 ± 0.006[g]
				4.160[c]	4.180 ± 0.001[j]
C_6 cyclic	2.46	2.66	2.87		
C_7 linear	3.33	3.37	3.42	2.95[a]	3.358 ± 0.014[g]
				3.265[d]	
C_7 cyclic	1.54	2.21	3.04		
C_8 linear	4.00	4.14	4.27	4.07[a]	4.379 ± 0.006[g]
				4.348[e]	
C_8 cyclic	1.72	2.55	2.51		
C_9 linear	3.60	3.66	3.72	3.21[a]	3.684 ± 0.010[g]
C_9 cyclic	2.90	3.20	3.22		
C_{10} linear	4.14	4.45	4.40	4.25[a]	
C_{10} cyclic	0.49	1.71	2.70		2.2 ± 0.1[g]
C_{11} cyclic	2.32	2.41	2.49		1.5 ± 0.1[g]
C_{12} cyclic	2.35	2.53	2.72		
C_{13} cyclic	3.28	3.43	3.50		

[a] Reference 24 (CCSD(T)/DZP+//ROHF/DZP results). [b] Reference 26 (CCSD(T)/pVTZ+//ROHF/DZP results). [c] Reference 27 (RCCSD(T)/288 cGTOs). [d] Reference 29 (RCCSD(T)/301 cGTOs). [e] Reference 28 (RCCSD(T)/272 cGTOs). [f] Oakes, J. M.; Ellison, G. B. *Tetrahedron* **1986**, *42*, 6263 (anion photoelectron spectroscopy). [g] Reference 5 (anion photoelectron spectroscopy). [h] Hong, X.; Miller, T. A. Private communication in ref 26 (anion photoelectron spectroscopy). [i] Algranati, M.; Feldman, H.; Kella, D.; Malkin, E.; Miklazky, E.; Naaman, R.; Vager, Z.; Zajfman, J. *Isr. J. Chem.* **1990**, *30*, 79 (Coulomb explosion imaging (CEI) technique). [j] Arnold, C.C; Zhao, Y.; Kitsopolous, T. N.; Neumark, D. M.; *J. Chem. Phys.* **1992**, *97*, 6121 (anion photoelectron spectroscopy).

their lowest unoccupied orbital (see section 3.3). For the odd-membered series, the lower adiabatic electron affinities are therefore quite naturally found for the polyynic C_7 and C_{11} rings. Among the even-membered rings, the minima of AEAs are reached with C_6 and C_{10}, which reflects the greater internal stability of these cumulenic clusters, whereas intrinsically more reactive polyynic species such as C_8 and C_{12} have larger AEA values. Therefore, the adiabatic electron affinities of carbon rings are reminiscent of the $4n$ periodicity that governs the alternation between cumulenic and polyynic systems and beautifully reflect the twisted and cumulenic nature of the anionic C_{4n+1}^- tori ($n = 1-3$).

4. Conclusions

In this paper, we report a thorough theoretical study of the structural, rotational, and vibrational properties of carbon cluster anions, in continuation of two previous studies on neutral carbon clusters and on the corresponding cations.[58,59] This work extensively employs density functional theory (DFT) and coupled-clusters (CC) theory in conjunction with the augmented cc-pVDZ basis set. The functional considered was B3LYP (Becke's three-parameter Lee−Yang−Parr). For the smaller chains, the obtained geometries are in line with calculations performed at higher theoretical levels, such as RCCSD(T). In this study, the impact of the diffuse functions in the basis set on the computed structures and properties has also been assessed. Bond lengths are practically unaffected by the inclusion of diffuse functions in the basis set, whereas substantial effects on the adiabatic electron affinities can be noted.

Most generally, the linear and merely cumulenic chains simply undergo a substantial increase of the bond-length alternation and a size increase upon adiabatic electron attachment, along with slight but significant distortions into noncentrosymmetric structures (C_5^-: C_s; C_7^-: C_2; C_8^-: C_{2v}; C_9^-: C_2,; C_{10}^-: C_2) because of strong Renner−Teller effects. We have noticed that *d* diffuse functions are essential for a sound description of all structural implications of such effects. Compared with the distortions seen with the carbon chains, the structural impacts of electron-attachment processes on carbon rings are far more varied and can be rationalized solely through a topological analysis of frontier orbitals. For both the linear and cyclic species, the computed IR spectra and rotational moments display specific markers of the structural variations introduced by electron attachment. The linear anions exhibit the most intense IR activity and show a systematically greater propensity to bind an extra electron than do the cyclic isomers. The strongest absorption region of the larger rings and chains lies between 1600 and 2200 cm^{-1}, which is in line with the experimental findings.

Closed anionic clusters such as C_5^-, C_9^-, and C_{13}^- are even-twisted cumulenic (i.e., aromatic) rings whose highest occupied levels are π orbitals that are characterized by a unique nodal surface showing an even number of 180° twists around the carbon ring. This peculiar and exquisite topology explains, among others, the overall limited alternation of bond lengths, the significant out-of-plane distortions at the B3LYP/aug-cc-pVDZ level, and the strikingly high electron affinity of the corresponding neutral clusters. Our calculations indicate the induction of particularly strong geometry relaxation effects during electron-attachment processes on the cyclic isomers of C_5, C_7, C_8, and C_{10} or during electron-detachment processes from the C_7^- and C_{10}^- rings. Therefore, it would certainly be worthwhile to extend the present study to detailed investigations of the vibronic fine structure at the electron-attachment threshold of cyclic carbon clusters or at the ionization threshold of the associated anions.

Acknowledgment. We acknowledge financial support from the Bijzonder Onderzoeksfonds (BOF) of the Limburgs Universitair Centrum and from the Fonds voor Wetenschappelijk Onderzoek van Vlaanderen, the Flemish Science Foundation (Belgium). All the calculations presented in this work have been run on two Alpha Digital workstations (models 533au2 and ES40) at the Limburgs Universitair Centrum.

References and Notes

(1) Weltner, W., Jr.; Van Zee, R. J. *Chem. Rev.* **1989**, *89*, 1713.
(2) Van Orden, A.; Saykally, R. J. *Chem. Rev.* **1998**, *98*, 2313.
(3) Yang, S. H.; Pettiette, C. L.; Conceicao, J.; Cheshnovsky, O.; Smalley, R. E. *Chem. Phys. Lett.* **1987**, *139*, 233.
(4) Yang, S. H.; Taylor, K. J.; Craycraft, M. J.; Conceicao, J.; Pettiette, C. L.; Cheshnovsky, O.; Smalley, R. E. *Chem. Phys. Lett.* **1988**, *144*, 431.
(5) Arnold, D. W.; Bradforth, S. E.; Kitsopoulos, T. N.; Neumark, D. M. *J. Chem. Phys.* **1991**, *95*, 8753.
(6) Handschuh, H.; Ganteför, G.; Kessler, B.; Bechthold, P. S.; Eberhardt, W. *Phys. Rev. Lett.* **1995**, *74*, 1095.
(7) Xu, C.; Burton, G. R.; Taylor, T. R.; Neumark, D. M. *J. Chem. Phys.* **1997**, *107*, 3428.
(8) Kohno, M.; Suzuki, S.; Shiromaru, H.; Moriwaki, T.; Achiba, Y. *Chem. Phys. Lett.* **1998**, *282*, 330.
(9) Ohara, M.; Kasuya, D.; Shiromaru, H.; Achiba, Y. *J. Phys. Chem. A* **2000**, *104*, 8622 and references therein.

(10) Zhao, Y.; de Beer, E.; Xu, C.; Taylor, T.; Neumark, D. M. *J. Chem. Phys.* **1996**, *105*, 4905.
(11) Szczepanski, J.; Ekern, S.; Vala, M. *J. Phys. Chem. A* **1997**, *101*, 1841.
(12) Szczepanski, J.; Wehlburg, C.; Vala, M. *J. Phys. Chem. A* **1997**, *101*, 7039.
(13) Szczepanski, J.; Vala, M.; Shen, L. N.; Withey, P. A.; Graham, W. R. M. *J. Phys. Chem. A* **1997**, *101*, 8788.
(14) Szczepanski, J.; Hodyss, R.; Vala, M. *J. Phys. Chem. A* **1998**, *102*, 8300.
(15) Maier, J. P. *J. Phys. Chem. A* **1998**, *102*, 3462 and references therein.
(16) Forney, D.; Fulara, J.; Freivogel, P.; Jakobi, M.; Lessen, D.; Maier, J. P. *J. Chem. Phys.* **1995**, *103*, 48.
(17) Freivogel, P.; Fulara, J.; Jakobi, M.; Forney, D.; Maier, J. P. *J. Chem. Phys.* **1995**, *103*, 54.
(18) Freivogel, P.; Grutter, M.; Forney, D.; Maier, J. P. *Chem. Phys.* **1997**, *216*, 401.
(19) Freivogel, P.; Grutter, M.; Forney, D.; Maier, J. P. *J. Chem. Phys.* **1997**, *107*, 4468.
(20) Wyss, M.; Grutter, M.; Maier, J. P. *Chem. Phys. Lett.* **1999**, *304*, 35.
(21) von Helden, G.; Kemper, P. R.; Gotts, N. G.; Bowers, M. T. *Science (Washington, D.C.)* **1993**, *259*, 1300.
(22) Jiao, C. Q.; Phelps, D. K.; Lee, S.; Huang, Y.; Freiser, B. S. *Rapid Commun. Mass. Spectrom.* **1993**, *7*, 404.
(23) Adamowicz, L. *J. Chem. Phys.* **1991**, *94*, 1241.
(24) Watts, J. D.; Bartlett, R. J. *J. Chem. Phys.* **1992**, *97*, 3445.
(25) Ortiz, J. V.; Zakrzewski, V. G. *J. Chem. Phys.* **1994**, *100*, 6614.
(26) Watts, J. D.; Bartlett, R. J. *J. Chem. Phys.* **1994**, *101*, 409.
(27) Schmatz, S.; Botschwina, P. *Chem. Phys. Lett.* **1995**, *235*, 5.
(28) Schmatz, S.; Botschwina, P. *Chem. Phys. Lett.* **1995**, *245*, 136.
(29) Schmatz, S.; Botschwina, P. *Int. J. Mass Spectrom. Ion Processes* **1995**, *149/150*, 621.
(30) Brown, S. T.; Rienstra-Kiracofe, J. C.; Schaefer, H. F., III. *J. Phys. Chem. A* **1999**, *103*, 4065.
(31) Cao, Z.; Peyerimhoff, S. D. *J. Phys. Chem. A* **2001**, *105*, 627.
(32) von Helden, G.; Palke, W. E.; Bowers, M. T. *Chem. Phys. Lett.* **1993**, *212*, 247.
(33) Lakin, N. M.; Pachkov, M.; Tulej, M.; Maier, J. P.; Chambaud, G.; Rosmus, P. *J. Chem. Phys.* **2000**, *113*, 9586.
(34) Pasqualini, E. E.; López, M. *Chem. Phys. Lett.* **2001**, *336*, 33.
(35) Cao, Z.; Peyerimhoff, S. D.; Grein, F.; Zhang, Q. *J. Chem. Phys.* **2001**, *115*, 2062.
(36) Adamowicz, L. *J. Chem. Phys.* **1990**, *93*, 6685.
(37) Watts, J. D.; Cernusak, I.; Bartlett, R. J. *Chem. Phys. Lett.* **1991**, *178*, 259.
(38) Ortiz, V. J. *J. Chem. Phys.* **1993**, *99*, 6716.
(39) Adamowicz, L. *Chem. Phys. Lett.* **1991**, *182*, 45.
(40) Ortiz, J. V. *J. Chem. Phys.* **1992**, *97*, 7531.
(41) Ortiz, J. V. *Chem. Phys. Lett.* **1993**, *216*, 319.
(42) Ohno, M.; Zakrzewski, V. G.; Ortiz, J. V.; von Niessen, W. *J. Chem. Phys.* **1997**, *106*, 3258.
(43) (a) Parr, R. G.; Yang, W. *Density-Functional Theory of Atoms and Molecules*; Oxford University Press: New York, 1989. (b) Koch, W.; Holthausen, M. C. *A Chemist's Guide to Density Functional Theory*; Wiley-VCH: Weinheim, Germany, 2001.
(44) Rösch, N.; Trickey, S. B. *J. Chem. Phys.* **1997**, *106*, 8940.
(45) Jarecki, A. A.; Davidson, E. R. *Chem. Phys. Lett.* **1999**, *300*, 44.
(46) Tschumper, G. S.; Schaefer, H. F., III. *J. Chem. Phys.* **1997**, *107*, 252.
(47) de Proft, F.; Geerlings, P. *J. Chem. Phys.* **1997**, *106*, 327.
(48) Curtiss, L. A.; Redfern, P. G.; Raghavachari, K.; Pople, J. A. *J. Chem. Phys.* **1998**, *109*, 42.
(49) Ernzerhof, M.; Scuseria, E. G. *J. Chem. Phys.* **1999**, *110*, 502.
(50) Ernzerhof, M.; Scuseria, E. G. *J. Chem. Phys.* **1999**, *111*, 91.
(51) de Oliveira, G.; Martin, J. M. L.; de Proft, F.; Geerlings, P. *Phys. Rev. A* **1999**, *103*, 1034.
(52) Galbraith, J. M.; Schaefer, H. F., III. *J. Chem. Phys.* **1996**, *105*, 862.
(53) Becke, A. D. *J. Chem. Phys.* **1993**, *98*, 5648.
(54) Lee, C.; Yang, W.; Parr, R. G. *Phys. Rev. B* **1988**, *37*, 785.
(55) Raghavachari, K.; Trucks, G. W.; Head-Gordon, M.; Pople, J. A. *Chem. Phys. Lett.* **1989**, *157*, 479.
(56) Hample, C.; Peterson, K.; Werner, H. J. *Chem. Phys. Lett.* **1992**, *190*, 1.
(57) Lee, T. J.; Scuseria, E. G. Achieving Chemical Accuracy with Coupled-Cluster Theory. In *Quantum Mechanical Electronic Structure Calculations with Chemical Accuracy;* Langhoff, S. R., Ed.; Kluwer Academic Publishers: Dordrecht, The Netherlands, 1995.
(58) (a) Martin, J. M. L.; El-Yazal, J.; François, J.-P. *Chem. Phys. Lett.* **1995**, *242*, 570. (b) Martin, J. M. L.; El-Yazal, J.; François, J.-P. *Chem. Phys. Lett.* **1996**, *252*, 9.
(59) Giuffreda, M. G.; Deleuze, M. S.; François, J.-P. *J. Phys. Chem. A* **1999**, *103*, 5137.
(60) Martin, J. M. L.; El-Yazal, J.; François, J.-P. *Mol. Phys.* **1995**, *86*, 1437.
(61) (a) Dunning, T. H., Jr. *J. Chem. Phys.* **1989**, *90*, 1007. (b) Kendall, R. A.; Dunning, T. H., Jr.; Harrison, R. J. *J. Chem. Phys.* **1992**, *96*, 6769. (c) Woon, D. E.; Dunning, T. H., Jr. *J. Chem. Phys.* **1993**, *98*, 1358.
(62) MOLPRO (version 98.1) is a package of ab initio programs written by Werner, H.-J.; Knowles, P. J. with contributions from Almlöf, J.; Amos, R. D.; Berning, A.; Cooper, D. L.; Deegan, M. J. O.; Dobbyn, A. J.; Eckert, F.; Elbert, S. T.; Hampel, C.; Lindh, R.; Lloyd, A. W.; Meyer, W.; Nicklass, A.; Peterson, K.; Pitzer, R.; Stone, A. J.; Taylor, P. R.; Mura, M. E.; Pulay, P.; Schütz, M.; Stoll, H.; Thorsteinsson, T. University of Birmingham: Birmingham, U.K., 1998.
(63) Frisch, M. J.; Trucks, G. W.; Schlegel, H. B.; Scuseria, G. E.; Robb, M. A.; Cheeseman, J. R.; Zakrzewski, V. G.; Montgomery, J. A., Jr.; Stratmann, R. E.; Burant, J. C.; Dapprich, S.; Millam, J. M.; Daniels, A. D.; Kudin, K. N.; Strain, M. C.; Farkas, O.; Tomasi, J.; Barone, V.; Cossi, M.; Cammi, R.; Mennucci, B.; Pomelli, C.; Adamo, C.; Clifford, S.; Ochterski, J.; Petersson, G. A.; Ayala, P. Y.; Cui, Q.; Morokuma, K.; Malick, D. K.; Rabuck, A. D.; Raghavachari, K.; Foresman, J. B.; Cioslowski, J.; Ortiz, J. V.; Stefanov, B. B.; Liu, G.; Liashenko, A.; Piskorz, P.; Komaromi, I.; Gomperts, R.; Martin, R. L.; Fox, D. J.; Keith, T.; Al-Laham, M. A.; Peng, C. Y.; Nanayakkara, A.; Gonzalez, C.; Challacombe, M.; Gill, P. M. W.; Johnson, B. G.; Chen, W.; Wong, M. W.; Andres, J. L.; Head-Gordon, M.; Replogle, E. S.; Pople, J. A. *Gaussian 98*, revision A.7; Gaussian, Inc.: Pittsburgh, PA, 1998.
(64) (a) Peierls, R. E. *Quantum Theory of Solids*; Clarendon Press: Oxford, U.K., 1955. (b) Walatka, V. V.; Labes, M. M.; Perlstein, J. H. *Phys. Rev. Lett.* **1973**, *31*, 1139. (c) Greene, L.; Street, G. B.; Suter, L. J. *Phys. Rev. Lett.* **1977**, *38*, 1305.
(65) Martin, J. M. L.; Taylor, P. R. *J. Phys. Chem.* **1996**, *100*, 6047 and references therein.
(66) Herzberg, G.; Teller, E. *Z. Phys. Chem., Abt. B* **1933**, *21*, 410.
(67) Renner, R. *Z. Phys.* **1934**, *92*, 172.
(68) Lee, T. J.; Fox, D. J.; Schaefer, H. F.; Pitzer, R. M. *J. Chem. Phys.* **1984**, *81*, 356.
(69) *The Fullerenes: New Horizons for the Chemistry, Physics, and Astrophysics of Carbon;* Kroto, H. W., Walton, D. R. M., Eds.; Cambridge University Press: Cambridge, U.K., 1993.
(70) Deleuze, M. S.; Giuffreda, M.-G.; François, J.-P. *J. Phys. Chem. A* **2002**, *106*, 5626.
(71) Trinajstic, N. *Chemical Graph Theory*, 2nd ed.; Mathematical Chemistry Series; CRC Press: Boca Raton, FL, 1992.
(72) Kemper, P R.; Bowers, M. T. *J. Phys. Chem.* **1991**, *95*, 5134
(73) Lee, T. J.; Taylor, P. R. *Int. J. Quantum Chem., Symp.* **1989**, *23*, 199.
(74) Martin, J. M. L.; Lee, T. J.; Scuseria, G. E.; Taylor, P. R. *J. Chem. Phys.* **1997**, *9*, 6549.